

# Stochastic embedding DFT: theory and application to p-nitroaniline in water

Wenfei Li,<sup>1</sup> Ming Chen,<sup>2</sup> Eran Rabani,<sup>2</sup> Roi Baer,<sup>3</sup> and Daniel Neuhauser<sup>1</sup>

<sup>1</sup>*Department of Chemistry and Biochemistry, University of California, Los Angeles California 90095, USA*

<sup>2</sup>*Affiliation: Department of Chemistry, University of California and Materials Science Division, Lawrence Berkeley National Laboratory, Berkeley, California 94720, USA*

<sup>3</sup>*Affiliation: Fritz Haber Center for Molecular Dynamics, Institute of Chemistry, The Hebrew University of Jerusalem, Jerusalem 91904, Israel*

(Dated: 20 May 2019)

Over this past decade, we combined the idea of stochastic resolution of identity with a variety of electronic structure methods. In our stochastic Kohn-Sham DFT method, the density is an average over multiple stochastic samples, with stochastic errors that decrease as the inverse square root of the number of sampling orbitals. Here we develop a stochastic embedding density functional theory method (se-DFT) that selectively reduces the stochastic error (specifically on the forces) for a selected sub-system(s). The motivation, similar to that of other quantum embedding methods, is that for many systems of practical interest the properties are often determined by only a small sub-system. In stochastic embedding DFT two sets of orbitals are used: a deterministic one associated with the embedded subspace, and the rest which is described by a stochastic set. The method is exact in the limit of large number of stochastic samples. We apply se-DFT to study a p-nitroaniline molecule in water, where the statistical errors in the forces on the system (the p-nitroaniline molecule) are reduced by an order of magnitude compared with non-embedding stochastic DFT.

DFT (Density Functional Theory) traditionally follows the Kohn-Sham scheme where a set of one-particle equations is solved self-consistently. For large systems the solution of these equations scales as  $O(N_e^2) - O(N_e^3)$  with the number of electrons  $N_e$ , so there is a lot of interest in variants that scale linearly with system size. Such methods include orbital-free DFT with density-dependent kinetic energy functionals,<sup>1,2</sup>; linear-scaling approaches where the system is split into parts that are woven together via constraints<sup>3</sup>; as well as embedding techniques where an inner part is treated by DFT and an outer part by orbital-free DFT<sup>4-6</sup>.

Previously, we developed stochastic DFT (sDFT), a method that can be viewed as a bridge between Kohn-Sham DFT and orbital-free DFT<sup>7</sup>. Instead of computing Kohn-Sham orbitals for all occupied states, we apply a Chebyshev filter to a few stochastic orbitals<sup>7</sup>, and extract the density from these filtered orbitals, circumventing the time-consuming diagonalization step. This approach is exact in the limit of infinitely many stochastic samples and gives useful results even for a small number of samplings.

In a follow-up work<sup>8-10</sup> we have shown how to reduce the standard deviation in sDFT (and therefore accelerate the convergence), using a method we label stochastic-fragment DFT (sf-DFT). Here, instead of sampling stochastically the full density, we sample stochastically only the difference between the full density and a zero-order density which is easy to calculate. The difference is generally small, thereby reducing the fluctuations.

Here, we develop an alternate method whereby a given sub-region is embedded. Essentially, this sub-region is treated deterministically while the rest of the system is treated stochastically (this is a simplifying view and the

more precise methodology is described later). The motivation for this method is that, for many realistic systems, only a subsystem is of particular importance. The idea of embedding was widely adopted to treat such systems. In most embedding methods, the sub-system of interest is calculated at higher level theories, while the rest is treated with less accurate but more efficient methods to reduce computational cost<sup>4,5,11-22</sup>. Our stochastic density functional theory embedding method adopts an analogous strategy, except that here the larger stochastic region embeds the smaller deterministic part.

An attractive feature of the stochastic embedding method is that the errors due to the embedding are numerically controlled, since in the limit of infinitely many stochastic samplings the method is exact. As such, there is no residual arbitrariness due to the choice of an embedding potential.

This paper is organized as follows. Sec. I presents the theory, and the practical algorithm is reviewed in Sec. II. In Sec. III a practical system is studied, embedding of a dye (p-nitroaniline) in 216 water molecules. Discussion and possible extensions follow in Sec. IV.

## I. THEORY

### A. Stochastic DFT

We first review stochastic DFT as developed in our previous works<sup>7,8,10,11</sup>.

In DFT, the key component is the electron density  $\rho(\mathbf{r})$ , which we express as the trace of a Heaviside step function:

$$\frac{\rho(\mathbf{r})}{2} = \langle \mathbf{r} | \Theta(\mu - H) | \mathbf{r} \rangle \quad (1)$$

where we assume spin-unpolarized DFT. Here,  $\mu$  is the electron chemical potential, determined by ensuring the correct total number of electrons:

$$N_e = \int \rho(\mathbf{r}) d\mathbf{r}, \quad (2)$$

and the one-body Hamiltonian is  $H = -\frac{1}{2}\nabla^2 + v(\mathbf{r})$ , where we introduced the is the effective one-electron potential due to the the nuclear ( $v_N$ ) electron-electron Coulomb interaction ( $v_H$ ) and exchange-correlation ( $v_{XC}$ ) parts. We assume for simplicity that the exchange-correlation (and therefore the total effective) potential depends on the local density,  $v = v[\rho]$ .

In the usual deterministic formulations of Kohn-Sham DFT, the electron density is expressed as the sum over one-electron states, and the total number of electrons is determined by the occupation number of each state. Thus, the Heaviside filter becomes a projection to the occupied subspace:

$$\Theta(\mu - H) = \sum_{i \leq N_{\text{occ}}} |\psi_i\rangle \langle \psi_i|. \quad (3)$$

where we introduced the number of occupied orbitals ( $N_{\text{occ}} = N_e/2$ ). The one-electron orbitals  $\psi_i$  are obtained by diagonalization of the effective one-electron Hamiltonian matrix, resulting in a nominal  $N_e^3$  scaling of Kohn-Sham DFT. Expectation values of one-electron operators are obtained from the occupied states:

$$\langle A \rangle = \sum_{i \leq N_{\text{occ}}} \langle \psi_i | A | \psi_i \rangle. \quad (4)$$

In stochastic Kohn-Sham DFT, on the other hand, we use a set of stochastic orbitals,  $\xi(r)$ , with the property that:

$$\{|\xi\rangle \langle \xi|\}_{\xi} = I, \quad (5)$$

where the curly brackets stand for averaging over all stochastic orbitals. Inserting the identity operator in the expression for  $\rho(\mathbf{r})$ , the electron density is thus expressible as:

$$\rho(\mathbf{r}) = \left\{ \langle \mathbf{r} | \Theta^{\frac{1}{2}} |\xi\rangle \langle \xi | \Theta^{\frac{1}{2}} | \mathbf{r} \rangle \right\}_{\xi} = \{ |\xi_{\mu}(\mathbf{r})|^2 \}_{\xi}, \quad (6)$$

where we abbreviate  $\Theta^{\frac{1}{2}} \equiv \Theta^{\frac{1}{2}}(\mu - H)$ , and  $\xi_{\mu} \equiv \Theta^{\frac{1}{2}} \xi$ .

The filtered stochastic orbitals are linear combinations of all occupied states with random coefficients:

$$\xi_{\mu}(\mathbf{r}) = \sum_{i \leq N_{\text{occ}}} c_i \phi_i(\mathbf{r}) \quad (7)$$

where  $c_i = \langle \phi_i | \xi \rangle$ , so

$$\{c_i^* c_j\} = \delta_{ij}. \quad (8)$$

Similarly, the expectation values of any one-particle operator  $D$  is:

$$\langle D \rangle = \{ \langle \xi_{\mu} | D | \xi_{\mu} \rangle \}_{\xi} \approx \frac{1}{N_s} \sum_{\xi} \langle \xi_{\mu} | D | \xi_{\mu} \rangle. \quad (9)$$

Here  $N_s$  is the number of stochastic orbitals used in practice. As in any stochastic method, the expectation value, obtained as the average of a finite number of samples, will have an associated stochastic error which is proportional to  $1/\sqrt{N_s}$ . The actual number of stochastic orbitals is chosen based on the required level of precision.

In practice the method relies on the fact that the calculation of each stochastic vector scales only linearly with system size. Specifically, we use a smooth Heaviside function,  $\Theta(\mu - H) = \frac{1}{2} \text{erfc}(\beta(\mu - H))$  where  $\beta$  needs to be much larger than the inverse band gap. The smooth theta function is then expressed as a finite sum of Chebyshev polynomials,  $\Theta^{\frac{1}{2}} = \sum_n a_n(\mu) T_n(H_{\text{scaled}})$ , where  $H_{\text{scaled}}$  is a scaled Hamiltonian with eigenvalues in the range  $[-1, 1]$  and  $a_n(\mu)$  are the Chebyshev coefficients of  $(\frac{1}{2} \text{erfc}(\beta(\mu - H)))^{\frac{1}{2}}$ . Therefore

$$|\xi_{\mu}\rangle = \sum_n a_n(\mu) |\xi^n\rangle, \quad (10)$$

where the Chebyshev vectors are obtained recursively,  $|\xi^n\rangle = 2H_{\text{scaled}}|\xi^{n-1}\rangle - |\xi^{n-2}\rangle$ , and  $|\xi^{n=0}\rangle \equiv |\xi\rangle$ .

The Chebyshev expansion makes it possible to analytically determine the chemical potential. Specifically, expand  $\Theta = \sum_n b_n(\mu) T_n(H_{\text{scaled}})$ , where  $b_n(\mu)$  are the Chebyshev coefficients of  $\frac{1}{2} \text{erfc}(\beta(\mu - H))$ . Then, using Eq. (2) gives:

$$\frac{N_e}{2} = \frac{1}{N_s} \sum_{\xi} \langle \xi_{\mu} | \Theta(\mu - H) | \xi_{\mu} \rangle = \sum_n b_n(\mu) R_n \quad (11)$$

where  $R_n = N_s^{-1} \sum_{\xi} \langle \xi | T_n(H_{\text{scaled}}) | \xi \rangle$ . Therefore,  $\mu$  is varied until Eq. (11) is fulfilled.

Next we turn to embedding, first traditional and then stochastic.

## B. DFT Embedding

As in other embedding methods, the motivation for stochastic DFT embedding is that in many practical applications the properties of a system depend on much smaller sub-system(s), such as defects in semiconductors or active sites of proteins. Often, we do not even care for the rest of the system except the embedded part. Even when a quantum-mechanical treatment of the rest of the system (the environment) is necessary, the level of precision required is usually not as high as that of the sub-system(s) of interest.

A key component in all types of embedding methods is the specific quantity through which the properties of the environment is conveyed to the sub-system(s). In DFT embedding, the quantity is the electron density of the entire system<sup>17</sup>. Specifically, subset A denotes the sub-system of interest, and subset B is associated with the environment (the precise meaning of these two subsets would be flexible). The total electron density is therefore partitioned  $\rho = \rho_A + \rho_B$ .

In traditional deterministic DFT embedding one then derives an approximate functional for the two regions that captures the energy of the environment as well as its interaction with the sub-system(s) of interest. Solving this equation for orbitals in subset A is equivalent to solving an ordinary Kohn-Sham equation with an extra external potential due to the embedding. There are different choices based on a requirement that the orbitals of the sub-system(s) should be orthogonal to the orbitals of the environment. In practice, this term can be approximated<sup>4,17</sup>, or the orthogonality can be incorporated explicitly<sup>11-14,23,24</sup>.

In our stochastic embedding DFT, there is the same loose overall goal as in deterministic embedding, i.e., the different treatment of a smaller system and the environment. However, the methods are quite different. In our approach, the embedded space is treated deterministically and the other (environment) is treated stochastically but otherwise the treatment is exact. Therefore, the only sense in which embedding is approximate here is numerical, i.e., if we use enough stochastic orbitals the results are exact. The two spaces (system and environment) see the same overall Hamiltonian, and there is no uncontrolled ansatz.

Specifically, using the same language of partitioning space to parts, we separate the total electron density into two parts, abbreviating

$$\begin{aligned} \frac{\rho(\mathbf{r})}{2} &= \langle \mathbf{r} | \Theta^{\frac{1}{2}} \Theta^{\frac{1}{2}} | \mathbf{r} \rangle \\ &= \langle \mathbf{r} | \Theta^{\frac{1}{2}} P \Theta^{\frac{1}{2}} | \mathbf{r} \rangle + \langle \mathbf{r} | \Theta^{\frac{1}{2}} Q \Theta^{\frac{1}{2}} | \mathbf{r} \rangle \\ &\equiv \frac{\rho_A(\mathbf{r})}{2} + \frac{\rho_B(\mathbf{r})}{2}. \end{aligned} \quad (12)$$

The first term in the splitting projects onto the ‘‘A’’ subspace, defined by its basis

$$\hat{P} = \sum_{i \in A} |\chi_i\rangle \langle \chi_i|, \quad \langle \chi_i | \chi_j \rangle = \delta_{ij}. \quad (13)$$

Therefore,

$$\frac{1}{2} \rho_A(\mathbf{r}) = \sum_{i \in A} \langle \mathbf{r} | \Theta^{\frac{1}{2}} | \chi_i \rangle \langle \chi_i | \Theta^{\frac{1}{2}} | \mathbf{r} \rangle = \sum_{i \in A} |\chi_{i,\mu}(\mathbf{r})|^2, \quad (14)$$

where  $\chi_{i,\mu} = \Theta^{\frac{1}{2}}(\mu - H)\chi_i$ . Note that the  $\chi_i(\mathbf{r})$  basis does not have to be related directly to the molecular orbitals but would typically be made from a set of atomic orbitals in a given region, although there is a lot of freedom in the definition. For example, in the example studied later we choose a set of local Gaussian atomic orbitals on each atom in the embedded subsystem (labeled as  $\phi_i(\mathbf{r})$ ,  $i \in A$ ) and then orthogonalize them, to produce  $\chi_i(\mathbf{r}) = \sum_j (S^{-\frac{1}{2}})_{ij} \phi_j(\mathbf{r})$  where  $S_{ij} = \langle \phi_i | \phi_j \rangle$  is the overlap matrix of the embedded-part atomic orbitals.

The second term in the splitting is associated with  $Q \equiv I - P$ , the orthogonal projection to the other (‘‘B’’) subspace. Since  $Q^2 = Q$  and inserting the identity operator  $I = \{|\xi\rangle \langle \xi|\}_\xi$  we get

$$\begin{aligned} \frac{1}{2} \rho_B(\mathbf{r}) &= \langle \mathbf{r} | \Theta^{\frac{1}{2}} Q Q \Theta^{\frac{1}{2}} | \mathbf{r} \rangle \\ &= \left\{ \langle \mathbf{r} | \Theta^{\frac{1}{2}} Q |\xi\rangle \langle \xi | Q \Theta^{\frac{1}{2}} | \mathbf{r} \rangle \right\}_\xi \\ &= \left\{ |\bar{\xi}_\mu(\mathbf{r})|^2 \right\}_\xi \end{aligned} \quad (15)$$

where

$$|\bar{\xi}_\mu\rangle \equiv \Theta^{\frac{1}{2}}(\mu - H)Q|\xi\rangle \quad (16)$$

is obtained by two consecutive projections: first a random orbital is projected to the space orthogonal to the embedded  $P$  part, and the result is then projected to the occupied space of the full system.

Thus we reach the main embedding expression, the separation of the density into two parts,

$$\frac{1}{2} \rho(\mathbf{r}) = \sum_{i \in A} |\chi_{i,\mu}(\mathbf{r})|^2 + \frac{1}{N_s} \sum_{\xi} |\bar{\xi}_\mu(\mathbf{r})|^2, \quad (17)$$

one associated with the deterministic subspace and one with an orthogonal stochastic part. The two parts are connected through the application of the density matrix operator,  $\Theta(\mu - H)$ , since the potential in the Hamiltonian depends on the density,  $v = v[\rho]$ , and the density is a mixture of stochastic and deterministic parts.

An important feature of the algorithm is that the deterministic and stochastic orbitals,  $\chi_{i\mu}$  and  $\bar{\xi}_\mu$ , that make

up the density (Eq. (17)), are not orthogonal – neither among themselves nor to each other. The orthogonality of the  $P$  and  $Q$  spaces reflects in the orthogonality of the original  $\chi_i$  and  $Q\xi$  functions, but that orthogonality is lost when we act on  $\chi_i$  and on  $Q\xi$  with  $\Theta^{\frac{1}{2}}(\mu - H)$  in Eqs. (14),(16). Further note that, as mentioned, the same overall Hamiltonian (and therefore the same  $\Theta^{\frac{1}{2}}(\mu - H)$ ) is used in preparing both the stochastic and deterministic orbitals, i.e., they are treated on equal footing.

## II. ALGORITHM

The overall stochastic embedding DFT method is then quite similar to the stochastic DFT algorithm:

1. Generate  $N_s$  stochastic orbitals:  $\xi(\mathbf{r}) = \pm 1/\sqrt{d^3r}$  where  $d^3r$  is the volume element associated with the grid. Also create a reasonable initial density  $\rho(\mathbf{r})$  which integrates to the correct number of valence electrons.
2. Determine the one-particle effective potential and Hamiltonian  $H = T + v[\rho]$
3. For each stochastic orbital, project out the components along the atomic basis functions, i.e., prepare  $\bar{\xi} = Q\xi$ :

$$\bar{\xi}(\mathbf{r}) = \xi(\mathbf{r}) - \sum_i c_i \chi_i(\mathbf{k})$$

where

$$c_i = \int \chi_i(\mathbf{r}) \xi(\mathbf{r}) d\mathbf{r}.$$

4. Determine the correct chemical potential  $\mu$  as the one that integrates correctly the total density, i.e., from Eq. (11) where now

$$R_n = \sum_{i \in A} \langle \chi_i | T_n (H_{\text{scaled}}) | \chi_i \rangle + \frac{1}{N_s} \sum_{\xi} \langle \bar{\xi} | T_n (H_{\text{scaled}}) | \bar{\xi} \rangle, \quad (18)$$

i.e., the residues and therefore the constraint on the integrated density include both the deterministic and stochastic parts.

5. Chebyshev filter the orthogonalized atomic basis functions as well as the projected stochastic functions:

$$|\chi_{i,\mu}\rangle = \Theta^{\frac{1}{2}}(\mu - H) |\chi_i\rangle$$

$$|\bar{\xi}_\mu\rangle = \Theta^{\frac{1}{2}}(\mu - H) |\bar{\xi}\rangle,$$

6. Calculate the charge densities for this  $\mu$  from Eq. (17).
7. Reiterate steps 2–6 until the density does not vary, i.e., SCF convergence is reached.

With the filtered atomic basis functions and filtered stochastic orbitals, the expectation value of any one-particle operator  $D$  is:

$$\langle D \rangle = \sum_i \langle \chi_{i,\mu} | D | \chi_{i,\mu} \rangle + \frac{1}{N_s} \langle \bar{\xi}_\mu | D | \bar{\xi}_\mu \rangle. \quad (19)$$

The algorithm is therefore very similar to the original stochastic DFT approach. The only differences are that (i) in addition to the stochastic functions one also needs to project the density matrix (or more precisely  $\Theta^{\frac{1}{2}}(\mu - H)$ ) on the deterministic basis making the embedded part, and (ii) for the stochastic part, we now project out the deterministic part (i.e., apply  $Q$ ) before filtering with the Chebyshev expansion of  $\Theta^{\frac{1}{2}}(\mu - H)$ .

## III. COMPUTATIONAL DETAILS

We applied the stochastic density functional embedding method to study a realistic case of embedding, i.e., a dye in water. The dye was a p-nitroaniline molecule, and it was embedded in 216 water molecules.

### A. Structure preparation

The configuration of the system was obtained from snapshots of molecular dynamic simulations with Gromacs 5<sup>25</sup>. The dynamics simulations used a generalized amber force field with charges from AM1-BCC for p-nitroaniline<sup>26</sup> and TIP4P with allowed flexibility of bond/bend for water<sup>27</sup>.

The simulation steps for the preparation of the configuration were standard, involving first a high temperature equilibrations of the p-nitroaniline, followed by NVT simulations at room temperature, and then NPT equilibration at room temperature and pressure. We then ran the MD sampled a specific configurations after several nsec. The configuration was used for subsequent DFT calculations and is shown in Figure 1.

### B. Stochastic embedding DFT details

For the DFT calculation, we imposed periodic boundary conditions. A plane wave expansion was used, with atomic norm-conserving Troullier-Martins pseudopotentials replacing the core-valence interaction. An LDA functional was used. An 88<sup>3</sup> grid with a spacing of 0.402 atomic units was used, while the plane wave kinetic-energy cutoff was 15 Hartree. The inverse-temperature-like parameter  $\beta$  in the Heaviside function  $\text{erfc}(\beta(\mu - H))$  was set at  $\beta = 0.03$  Hartree<sup>-1</sup>, requiring 1173 Chebyshev propagations in acting with  $\Theta^{\frac{1}{2}}(\mu - H)$ .

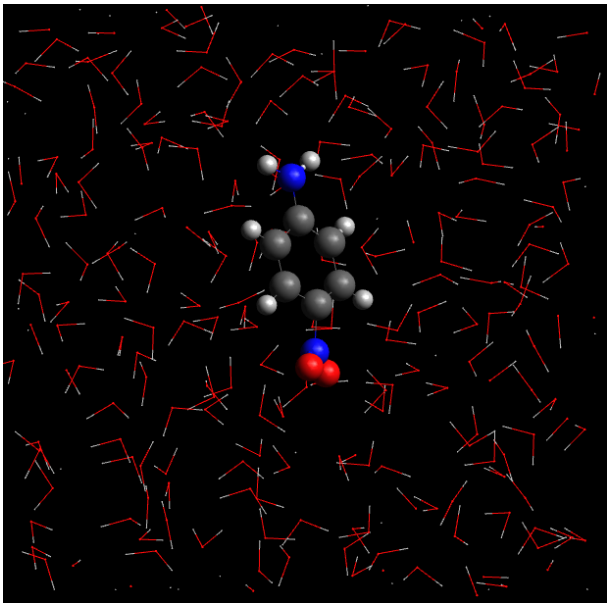


FIG. 1: Configuration of the p-nitroaniline/water system used in DFT calculation. The p-nitroaniline molecule is represented by ball and sticks, and water molecules are represented by wire-frames.

For the embedding basis sets we used a Gaussian double-zeta basis optimized for pseudopotentials, as given in the Quickstep<sup>28</sup> data set.<sup>29</sup>

Three sets of calculations were carried out. The first used  $N_s = 96$  stochastic orbitals, without embedding. The second used the same  $N_s = 96$  stochastic functions, but supplemented them with the double zeta atomic basis set for all 16 atoms belonging to the p-nitroaniline molecule. This deterministic basis set for the dye contained 160 functions (an average of 10 functions per atom). The atomic functions were orthogonalized, giving rise to 160 orthogonal  $\chi_i(\mathbf{r})$  functions. Therefore a total of 256 functions was employed (160 deterministic and 96 stochastic).

Since the number of deterministic functions in the second, embedded, set of calculations was quite large, we also compared the second set with a third set where all functions were stochastic, and where 256 functions were used, i.e., the same overall number as in the second set. Thus, the numerical effort, mostly associated with the Chebyshev application of  $\Theta^{\frac{1}{2}}$ , is similar in the second and third sets.

Each set of calculations was repeated ten times, with different random seeds for generating the stochastic orbitals, to obtain the standard deviation of the stochastic approaches.

To benchmark our results, we also performed a conventional deterministic Kohn-Sham DFT calculation which matches the results of Quantum-Espresso.<sup>30</sup>

	$N_s = 96$ without embedding	$N_s = 96$ with embedding	$N_s = 256$ without embedding	Deterministic
Total energy per electron	$-2.115 \pm 0.0015$	$-2.115 \pm 0.0016$	$-2.117 \pm 0.0008$	-2.117
Hartree energy per electron	$1.098 \pm 0.0023$	$1.098 \pm 0.0025$	$1.100 \pm 0.0016$	1.103
Exchange-correlation energy per electron	$-0.521 \pm 0.0004$	$-0.521 \pm 0.0004$	$-0.521 \pm 0.0002$	-0.522

TABLE I: DFT energies per electron, in Hartree. For the stochastic calculations, the energies were obtained as average of ten calculations, and the standard deviation is included. As clearly seen, embedding does not affect the accuracy of the overall energies.

#### IV. RESULTS

The most time-consuming step in the stochastic DFT formulation is the application of the Chebyshev filter. Therefore, as mentioned, the time required to perform calculation with embedding and  $N_s = 96$  (second set) is comparable to that with no embedding and  $N_s = 256$  (third set), and is about 2.5 times the time required to perform calculation with no embedding and  $N_s = 96$  (first set). Indeed, in practice about 14 core hours per SCF iteration (on a cluster with 2.5 GHz nodes) were needed for the second and third sets, with about 6 core hours for the first set. The deterministic set required about 11 core hours per iterations. In all cases, 30 DIIS iterations were used for full SCF convergence.

Next, we compared the total energy per electron obtained from the three sets of calculations with that obtained from the deterministic calculation, as well as the individual contribution from Hartree and exchange-correlation energies. The comparison is shown in Table I. The results show good overall agreement between the stochastic and deterministic calculations. Most importantly the standard deviations of energies is not affected by embedding, because the dominant contribution comes from the 216 water molecules. The standard deviation decreases of course by increasing  $N_s$ .

The effect of embedding comes to play in quantities relating to the embedded region, and the main such quantity is the force on each atom. Figure 2 shows the overall forces and their standard deviations for 60 out of the 644 atoms in the sample; the first 16 are the embedded dye, and the other 44 are from the water molecules. The figure clearly shows that, with embedding, the forces on the embedded atoms have much higher accuracy (much smaller standard deviation) than the forces on the water molecule.

As a side remark note that the forces on the non-embedded atoms have the same overall statistical fluctuation.

	$N_s = 96$ without embedding	$N_s = 96$ with embedding	$N_s = 256$ without embedding
Average over embedded atoms	1.92	0.20	1.54
Average over other atoms	2.23	2.22	1.47

TABLE II: Average standard deviations of the atomic force magnitudes, in eV/Å.

tuations as without embedding. We know from previous studies that for large systems like the present one the stochastic errors are independent of size, and depend only on the number of stochastic samples. Thus, the approach presented here would not deteriorate with the overall size of the full system.

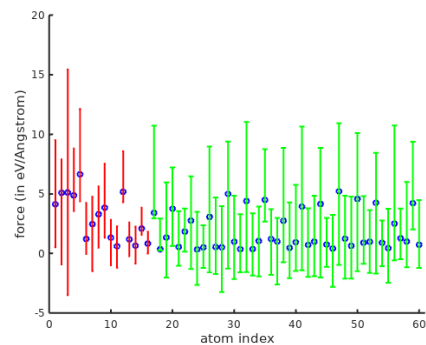
Coming back to the embedded system (the dye), the higher accuracy on the dye forces is shown more quantitatively in Table II, where the standard deviations of the forces on the dye is an order of magnitude smaller than for water molecules.

The results show that embedding significantly reduces the stochastic error of the accelerations for the selected (i.e., embedded) atoms. As expected, when the same number of stochastic orbitals is used, the standard deviation averaged over the non-embedded atoms remains the same. Meanwhile, due to the good description of the embedded atoms by the deterministic atomic basis, the standard deviations of the forces for those atoms decrease by one order of magnitude relative to the no-embedding case. To achieve without embedding the same level of accuracy in the forces, we will need 10,000 stochastic orbitals, which would be very time consuming.

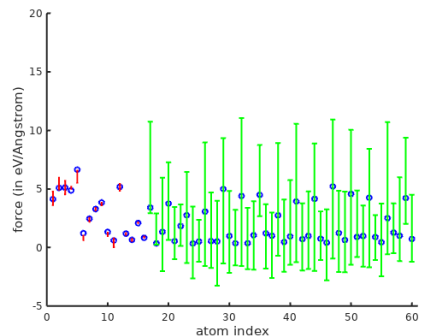
## V. SUMMARY AND PROSPECTS

In summary, we presented a stochastic embedding DFT method (se-DFT) that significantly reduces the statistical errors in the forces for the selected subgroup of atoms (i.e., the embedded atoms). Combined with the favorable linear scaling of stochastic DFT, the method can be applied to large systems of practical interests. Of course, as it stands the method is not efficient for overall MD of the full system, due to the large stochastic errors on the environment (i.e., non-embedded) atoms; rather it is suitable for applications where information on a selected region is desired.

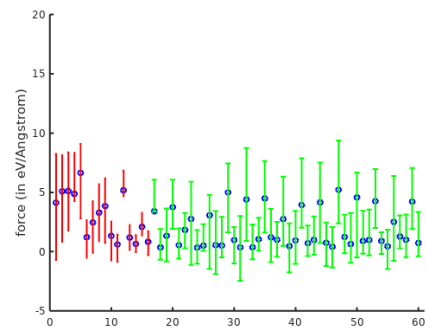
The embedding approach presented here is very general and can be extended in several directions. First, here we used an embedded space made from low-level atomic basis functions; we can replace it by a more general higher level basis. Further, we could economize and choose in the  $P$  basis only occupied eigenfunctions of the embedded part in, e.g., a dielectric medium. There will be occasions where the best basis would be energy selec-



(a)  $N_s = 96$ , without embedding



(b)  $N_s = 96$ , with embedding



(c)  $N_s = 256$ , without embedding

FIG. 2: Forces and their standard deviations for 60 (out of the 664 overall) atoms, in eV/Å. The first 16 atoms in the plot are the p-nitroaniline molecule, and the other 44 are from water molecules. In the second set, the atoms of the p-nitroaniline are embedded, and in the first and third set they are not. The blue circles denote the forces calculated by deterministic DFT, while the center of each bar refers to the average stochastic force. Red error bars are associated with the atoms of the p-nitroaniline molecule, and green bars are used for the standard deviation of the forces on the water atoms.

tive, i.e., a few energy-selective molecular eigenfunctions or a few energy selective eigenfunctions from a large cluster would be best used.

A second direction is a combination of embedding with our previous overlapping fragment technique (sf-DFT). That method reduces the statistical error of stochastic

DFT calculations<sup>8,9</sup> for all atoms, typically by up to an order of magnitude; specifically, instead of stochastically sampling the full density, we sample the difference between the full density and a zeroth-order density,  $\rho(\mathbf{r})$  which is a solution of a simple zeroth-order Hamiltonian  $H_0$  (e.g., that of overlapping fragments). Specifically:

$$\rho(\mathbf{r}) = \rho_0(\mathbf{r}) + \left\{ |\langle \mathbf{r} | \Theta^{\frac{1}{2}} | \xi \rangle|^2 - |\langle \mathbf{r} | \Theta_0^{\frac{1}{2}} | \xi \rangle|^2 \right\}_\xi, \quad (20)$$

where  $\Theta_0 \equiv \Theta(\mu_0 - H_0)$  and  $\mu_0$  is arbitrary. It is clear that this overlapping-fragment definition can be further extended by inserting projection operators as done earlier in the paper for the original stochastic DFT method. In a future paper we will examine whether a combination of overlapping fragments with embedding (i.e., combining se-DFT with sf-DFT) reduces the errors in the forces of the embedded part even further than either method alone.

A third direction is for methods other than DFT. For example embedding is applicable for the sub-linear scaling stochastic TDDFT method developed by us<sup>31</sup>. It is straightforward to see that the main embedding equation, Eq. (17), follows straightforwardly to TDDFT except that now all quantities (the density and the deterministic and stochastic orbitals) are time dependent. Such a time-dependent method has the desired property that the same Hamiltonian guides both the deterministic and stochastic function. An embedding-TDDFT method would be applicable to study the change in optical properties of chromophores due to the presence of solvent molecules, where we can use only a few stochastic orbitals to sample the solvent molecules, while the chromophore will be treated with embedding. This direction would be explored in a future paper.

## ACKNOWLEDGMENTS

D.N. acknowledges support from the NSF, Grant CHE-1763176. E.R. acknowledges support from the Department of Energy, Photonics at Thermodynamic Limits Energy Frontier Research Center, under grant number de-sc0019140. R.B. acknowledges support from the US-Israel Binational Science foundation under the BSF-NSF program, Grant No. 2015687.

The work also used resources of the National Energy Research Scientific Computing Center (NERSC), a U.S. Department of Energy Office of Science User Facility operated under Contract No. DE-AC02-05CH11231. The calculations were performed as part of the XSEDE<sup>32</sup> computational Project No. TG-CHE170058.

## APPENDIX

Here we give a simple demonstration of why embedding should improve the statistics. Say that the overall

problem has two spaces that are essentially separate, so each eigenstate  $\phi_i$  belongs to either the  $A$  or  $B$  subspaces. we choose the  $P$  subspace spanned by  $\{\chi_i : i \in A\}$  such that it is close to the subspace spanned by states in  $A$ :

$$P|\phi_i\rangle \simeq c_i^o|\phi_i\rangle, \quad (21)$$

where

$$c_i^o \approx \begin{cases} 1 & i \in A \\ 0 & i \in B \end{cases}. \quad (22)$$

The projected filtered stochastic orbital  $\bar{\xi}_\mu(\mathbf{r})$  is then given by a linear combination:

$$\bar{\xi}_\mu(\mathbf{r}) = \sum_{i \leq N_{Occ}} (c_i - c_i^o) \phi_i(\mathbf{r}). \quad (23)$$

For states belonging to  $A$ , instead of sampling  $c_i$  we are sampling  $(c_i - c_i^o)$  with average  $(1 - c_i^o) \approx 0$  and a much smaller standard deviation.

- <sup>1</sup>William C. Witt, Beatriz G. del Rio, Johannes M. Dieterich, and Emily A. Carter. Orbital-free density functional theory for materials research. *Journal of Materials Research*, 33(07):777–795, 2018.
- <sup>2</sup>Jouko Lehtomäki, Ilja Makkonen, Miguel A. Caro, Ari Harju, and Olga Lopez-Acevedo. Orbital-free density functional theory implementation with the projector augmented-wave method. *Journal of Chemical Physics*, 141(23), 2014.
- <sup>3</sup>Tai-Sung Lee, James P Lewis, and Weitao Yang. Linear-scaling quantum mechanical calculations of biological molecules: The divide-and-conquer approach. *Computational Materials Science*, 12(3):259–277, 1998.
- <sup>4</sup>Tomasz Adam Wesolowski and Arieh Warshel. Frozen density functional approach for ab initio calculations of solvated molecules. *The Journal of Physical Chemistry*, 97(30):8050–8053, 1993.
- <sup>5</sup>Tomasz A Wesolowski, Sapana Shedge, and Xiuwen Zhou. Frozen-density embedding strategy for multilevel simulations of electronic structure. *Chemical reviews*, 115(12):5891–5928, 2015.
- <sup>6</sup>Marcella Iannuzzi, Barbara Kirchner, and Jürg Hutter. Density functional embedding for molecular systems. *Chemical physics letters*, 421(1-3):16–20, 2006.
- <sup>7</sup>Roi Baer, Daniel Neuhauser, and Eran Rabani. Self-averaging stochastic kohn-sham density-functional theory. *Physical Review Letters*, 111(10):1–5, 2013.
- <sup>8</sup>Daniel Neuhauser, Roi Baer, and Eran Rabani. Communication: Embedded fragment stochastic density functional theory, 2014.
- <sup>9</sup>Eitam Arnon, Eran Rabani, Daniel Neuhauser, and Roi Baer. Equilibrium configurations of large nanostructures using the embedded saturated-fragments stochastic density functional theory. *The Journal of chemical physics*, 146(22):224111, 2017.
- <sup>10</sup>Ming Chen, Roi Baer, Daniel Neuhauser, and Eran Rabani. Overlapped embedded fragment stochastic density functional theory for covalently-bonded materials. *The Journal of chemical physics*, 150(3):034106, 2019.
- <sup>11</sup>Frederick R. Manby, Martina Stella, Jason D. Goodpaster, and Thomas F. Miller. A simple, exact density-functional-theory embedding scheme. *Journal of Chemical Theory and Computation*, 8(8):2564–2568, 2012. PMID: 22904692.

- <sup>12</sup>Patrick K. Tamukong, Yuriy G. Khait, and Mark R. Hoffmann. Density differences in embedding theory with external orbital orthogonality. *Journal of Physical Chemistry A*, 118(39):9182–9200, 2014.
- <sup>13</sup>Bence Hégyely, Péter R Nagy, György G Ferenczy, and Mihály Kállay. Exact density functional and wave function embedding schemes based on orbital localization. *The Journal of Chemical Physics*, 145(6):64107, 2016.
- <sup>14</sup>Tanner Culpitt, Kurt R Brorsen, and Sharon Hammes-Schiffer. Communication: Density functional theory embedding with the orthogonality constrained basis set expansion procedure. *The Journal of chemical physics*, 146(21):211101, 2017.
- <sup>15</sup>Andre Severo Pereira Gomes, Christoph R Jacob, and Lucas Visscher. Calculation of local excitations in large systems by embedding wave-function theory in density-functional theory. *Physical Chemistry Chemical Physics*, 10(35):5353–5362, 2008.
- <sup>16</sup>Daniele Loco, Louis Lagardère, Stefano Caprasecca, Filippo Lipparini, Benedetta Menucci, and Jean-Philip Piquemal. Hybrid QM/MM molecular dynamics with AMOEBA polarizable embedding. *Journal of chemical theory and computation*, 13(9):4025–4033, 2017.
- <sup>17</sup>Qiming Sun and Garnet Kin-Lic Chan. Quantum embedding theories. *Accounts of chemical research*, 49(12):2705–2712, 2016.
- <sup>18</sup>Tomasz A Wesolowski and Andreas Savin. Non-additive kinetic energy and potential in analytically solvable systems and their approximated counterparts. In *Recent progress in orbital-free density functional theory*, pages 275–295. World Scientific, 2013.
- <sup>19</sup>Jason D Goodpaster, Nandini Ananth, Frederick R Manby, and Thomas F Miller III. Exact nonadditive kinetic potentials for embedded density functional theory. *The Journal of chemical physics*, 133(8):084103, 2010.
- <sup>20</sup>Jason D Goodpaster, Taylor A Barnes, and Thomas F Miller III. Embedded density functional theory for covalently bonded and strongly interacting subsystems. *The Journal of chemical physics*, 134(16):164108, 2011.
- <sup>21</sup>Samuel Fux, Christoph R Jacob, Johannes Neugebauer, Lucas Visscher, and Markus Reiher. Accurate frozen-density embedding potentials as a first step towards a subsystem description of covalent bonds. *The Journal of chemical physics*, 132(16):164101, 2010.
- <sup>22</sup>David Schnieders and Johannes Neugebauer. Accurate embedding through potential reconstruction: A comparison of different strategies. *The Journal of chemical physics*, 149(5):054103, 2018.
- <sup>23</sup>Yuriy G Khait and Mark R Hoffmann. On the Orthogonality of Orbitals in Subsystem Kohn–Sham Density Functional Theory. In *Annual Reports in Computational Chemistry*, volume 8, pages 53–70. Elsevier, 2012.
- <sup>24</sup>Patrick K Tamukong, Yuriy G Khait, and Mark R Hoffmann. Accurate Dissociation of Chemical Bonds Using DFT-in-DFT Embedding Theory with External Orbital Orthogonality. *The Journal of Physical Chemistry A*, 121(1):256–264, 2016.
- <sup>25</sup>Herman J C Berendsen, David van der Spoel, and Rudi van Drunen. GROMACS: a message-passing parallel molecular dynamics implementation. *Computer physics communications*, 91(1-3):43–56, 1995.
- <sup>26</sup>Junmei Wang, Romain M Wolf, James W Caldwell, Peter A Kollman, and David A Case. Development and testing of a general amber force field. *Journal of computational chemistry*, 25(9):1157–1174, 2004.
- <sup>27</sup>William L Jorgensen and Jeffrey D Madura. Temperature and size dependence for Monte Carlo simulations of TIP4P water. *Molecular Physics*, 56(6):1381–1392, 1985.
- <sup>28</sup>Joost VandeVondele, Matthias Krack, Fawzi Mohamed, Michele Parrinello, Thomas Chassaing, and Jürg Hutter. Quickstep: Fast and accurate density functional calculations using a mixed gaussian and plane waves approach. *Computer Physics Communications*, 167(2):103–128, 2005.
- <sup>29</sup>We specifically used the DZVP-GTH-PADE basis for all atoms, in the CONFINED variant where available. The basis set is available from [https://github.com/SINGROUP/pycp2k/blob/master/examples/BASIS\\_SET](https://github.com/SINGROUP/pycp2k/blob/master/examples/BASIS_SET).
- <sup>30</sup>Paolo Giannozzi, Oliviero Andreussi, Thomas Brumme, Oana Bunau, M Buongiorno Nardelli, Matteo Calandra, Roberto Car, Carlo Cavazzoni, Davide Ceresoli, Matteo Cococcioni, et al. Advanced capabilities for materials modelling with quantum espresso. *Journal of Physics: Condensed Matter*, 29(46):465901, 2017.
- <sup>31</sup>Yi Gao, Daniel Neuhauser, Roi Baer, and Eran Rabani. Sublinear scaling for time-dependent stochastic density functional theory. *The Journal of chemical physics*, 142(3):34106, 2015.
- <sup>32</sup>John Towns, Timothy Cockerill, Maytal Dahan, Ian Foster, Kelly Gathier, Andrew Grimshaw, Victor Hazlewood, Scott Lathrop, Dave Lifka, Gregory D Peterson, and Others. XSEDE: accelerating scientific discovery. *Computing in Science & Engineering*, 16(5):62–74, 2014.